Thermal lensing analysis of TGG and its effect on beam quality

Amir A Jalali,* James Rybarsyk, and Evan Rogers
Electro-Optics Technology Inc., 5835 Shugart Lane, Traverse City, Michigan 49684, USA
*ajalali@eotech.com

Abstract: An analysis is presented of a TGG crystal rod under high power laser operation. A semianalytical thermal analysis is investigated to obtain the temperature profile and thermal lensing effect in a TGG crystal upon incidence of a high power laser light. By solving the heat transfer equation for the TGG crystal and taking the Gaussian beam transverse intensity profile as the heat source, the optical path difference due to induced thermal effects was obtained. Moreover, a detailed model for the dependence of thermal lensing and beam degradation which takes into account up to the fifth-order spherical aberration is presented. Based on this model, it is shown that up to a critical value of the beam power the degradation of the beam is not significant. The experimental results on thermal lensing and degradation on beam quality of a high power laser passing through a TGG crystal rod are in agreement with the main results from our model.

OCIS codes: (120.6810) Thermal effects; (260.2710) Inhomogeneous optical media; (260.1180) Crystal optics.

References and links

1. U. O. Farrukh, A. M. Buoncristiani, and C. E. Byvik, "An analysis of the temperature distribution in finite solid-state laser rods," IEEE J. Quantum Electron. **24**, 2253–2263 (1988).
2. M. Innocenzi, H. Yura, C. Fincher, and R. Fields, "Thermal modeling of continuous-wave end-pumped solid-state lasers," Appl. Phys. Lett. **56**, 1831–1833 (1990).
3. C. Pfistner, R. Weber, H. P. Weber, S. Merazzi, and R. Gruber, "Thermal beam distortions in end-pumped Nd:YAG, Nd:GSGG, and Nd:YLF rods," IEEE J. Quantum Electron. **30**, 1605–1615 (1994).
4. S. Fan, X. Zhang, Q. Wang, S. Li, S. Ding, and F. Su, "More precise determination of thermal lens focal length for end-pumped solid-state lasers," Opt. Commun. **266**, 620–626 (2006).
5. P. Shi, W. Chen, L. Li, and A. Gan, "Semianalytical thermal analysis of thermal focal length on Nd:YAG rods," Appl. Opt. **46**, 6655–6661 (2007).
6. E. Khazanov, N. Andreev, A. Babin, A. Kiselev, O. Palashov, and D. H. Reitze, "Suppression of self-induced depolarization of high-power laser radiation in glass-based Faraday isolators," J. Opt. Soc. Am. B **17**, 99–102 (2000).
7. E. Khazanov, N. Andreev, A. Mal'shakov, O. Palashov, A. Poteomkin, A. Sergeev, A. Shaykin, V. Zelenogorsky, I. Ivanov, R. Amin, G. Mueller, D. Tanner, and D. Reitze, "Compensation of thermally induced modal distortions in Faraday isolators," IEEE J. Quantum Electron. **40**, 1500–1510 (2004).
8. V. Zelenogorsky, O. Palashov, and E. Khazanov, "Adaptive compensation of thermally induced phase aberrations in Faraday isolators by means of a DKDP crystal," Opt. Commun. **278**, 8–13 (2007).
9. The Vigro Collaboration, "In-vacuum optical isolation changes by heating in a faraday isolator," Appl. Opt. **47**, 5853–5861 (2008).
10. A. E. Siegman, "Analysis of laser beam quality degradation caused by quartic phase aberrations," Appl. Opt. **32**, 5893–5901 (1993).
11. J. Alda, "Quality improvement of a coherent and aberrated laser beam by using an optimum and smooth pure phase filter," Opt. Commun. **192**, 199–204 (2001).
12. C. J. Kennedy, "Model for variation of laser power with M^2," Appl. Opt. **41**, 4341–4346 (2002).

#186287 - $15.00 USD Received 4 Mar 2013; revised 8 May 2013; accepted 10 May 2013; published 31 May 2013

13. J. Alda, *Laser and Gaussian Beam Propagation and Transformation* (Marcel Dekker, Inc, 2003), pp. 999–1013, Encyclopedia of Optical Engineering.
14. W. Koechner, *Solid State Laser Engineering* (Springer, 1988).
15. Y. Chen, T. Huang, C. Kao, C. Wang, and S. Wang, "Optimization in scaling fiber-coupled laser-diode end-pumped lasers to higher power: influence of thermal effect," IEEE J. Quantum Electron. 33, 1424–1429 (1997).
16. V. N. Mahajan, "Strehl ratio of a Gaussian beam," J. Opt. Soc. Am. A **22**, 1824–1833 (2005).
17. M. A. Porras, J. Alda, and E. Bernabeu, "Complex beam parameter and ABCD law for non-Gaussian and non-spherical light beams," Appl. Opt. **31**, 6389–6402 (1992).
18. R. J. Noll, "Zernike polynomials and atmospheric turbulence," J. Opt. Soc. Am. **66**, 207–211 (1976).
19. *NanoModeScan operational manual* (Photon Inc,*www.ophiropt.com*, 2008).

1. Introduction

While lasers are rapidly gaining acceptance in industrial and military markets, the problem of thermal lensing due to thermal effects in laser crystals has been of critical importance and investigated by numerous authors and researchers. [1–5] The high gain typically present in lasers makes Faraday isolators an essential component to prevent parasitic lasing between amplifying stages and external reflections back into their output. The thermal lensing effect of high power lasers is also an issue for optical isolator crystals especially when the beam is focused to a small area. Terbium gallium garnet (TGG), a commonly used Faraday crystal in the optical isolator community, shows low optical absorption in the near IR range and several orders of magnitude lower absorption than typical laser crystals. However, the requirements of small beam diameters in high power lasers leads to a thermal focal shift in the crystal due to the thermal lensing effect. On the other hand, other thermal effects such as thermal induced birefringence and Verdet constant temperature dependency would also be problematic in designing high power Faraday isolators. Attempts to overcome these issues have been extensively investigated by several groups and researchers. [6–9]

Heat generated within the TGG crystal leads to spatial variation of temperature and consequently results in a nonuniform phase difference of the beam traveling inside the crystal. This raises the problem of highly aberrated mediums in which the paraxial approach fails. In the case of aberration we may encounter the degradation in beam quality. [10] It is thus important to know how thermal effects will degrade the beam quality of TGG crystals in optical isolators for high power applications.

In this paper, we address the thermal lensing in edge-air-cooled TGG rod crystals and obtain thermal focal length in the crystal. In addition, we studied the degradation of a Gaussian beam passing through TGG crystals with fifth order thermal lens aberration due to thermal effects on the crystal. We derive an analytical formulation for the beam degradation based on the beam quality factor, "M-squared" method, the most mathematically rigorous and accepted method to characterize an arbitrary laser beam. [10–13]

2. Theoretical background

A schematic diagram of thermal analysis of a TGG crystal incident by a high power laser up to 310 W is shown in Fig. 1. The radius and the length of the crystal are represented as a and L, respectively. The crystal is coated on its end faces and reflectivity of incident light is less than 0.5%. The sides of the crystal are attached to a heat-sink and air cooled. A laser light of Gaussian profile with a wavelength of 1064 nm is incident on the center of the crystal rod. The light travels inside the crystal and deposits its energy into the crystal. A suitable beam size is chosen so that the Rayleigh range of the beam is much greater than the crystal length.

The laser light passes through an optical system consisting of a fiber ferrule and a collimating lens which focuses the beam waist on the axis of the crystal. Assuming the crystal rod end faces are located at $z = 0$ and at $z = L$, the light intensity is expressed by a Gaussian profile,

#186287 - $15.00 USD Received 4 Mar 2013; revised 8 May 2013; accepted 10 May 2013; published 31 May 2013

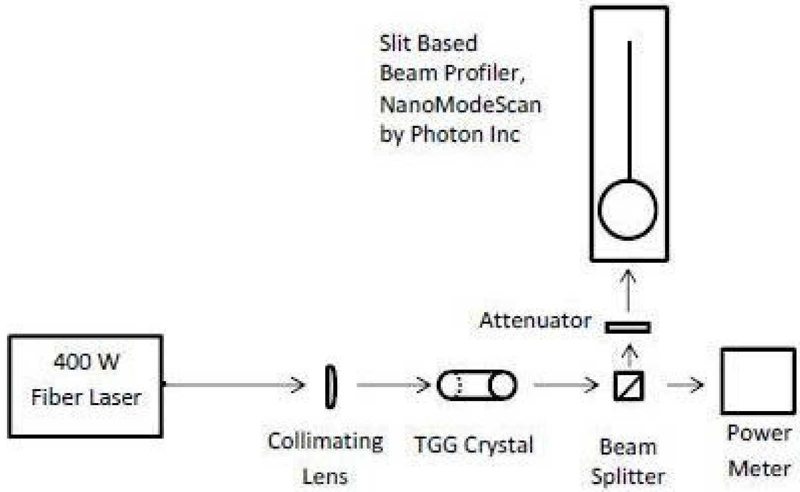

Fig. 1. Schematic diagram of the experimental setup for M^2 measurement

$I(r,z) = I_0 \exp(-2r^2/\omega^2(z)) \exp(-\alpha z)$, where I_0 is the intensity of light at origin (where light enters to the center of the crystal). The $1/e^2$ radius of Gaussian beam is shown by ω. In terms of Rayleigh range, $z_R = \pi\omega_0^2/\lambda$, it is expressed as

$$\omega^2(z) = \omega_0^2\left(1 + \frac{z^2}{z_R^2}\right), \tag{1}$$

where ω_0 and λ are the minimum spot size and the wavelength of the incident light, respectively. As light travels inside the crystal medium, its energy is absorbed by the medium and according to the absorption law the light intensity weakens exponentially through absorption coefficient α. The temperature difference is given by the solution for the steady state heat equation in cylindrical geometry and it is represented as the expansion of the radial and axial eigenstates with azimuthal symmetry.

$$T(r,z) \quad = \quad \sum_{n,l} A_{nl} J_0(\nu_n r/a)\ \sin(\lambda_l z + \beta_l), \tag{2}$$

where ν_n, the eigenvalues of radial equation, is the n-th zero of Bessel function of order zero $J_0(\nu_n r/a)$. λ_l and β_l are eigenvalues of axial equation. In obtaining Eq. (2) we assumed zero temperature on TGG rod surface and adiabatic boundary condition on two crystal ends. Zero temperature on the surface of the crystal rod indicates that we are calculating the rise in temperature relative to its value on the surface. The coefficients of expansion $A_{n,l}$ contain material and beam parameters and are obtained by integrals over the spatial distribution of heat generated by the incident light [1, 5]. The temperature profile represented in Eq. (2) for a TGG crystal rod is a general solution of the heat equation and is not limited to a Gaussian profile of the incident light. One can replace the incident Gaussian beam with an arbitrary beam intensity profile and solve for coefficients of expansion $A_{n,l}$.

3. Thermal focal length modeling

A laser source from SPI Lasers redPOWER with maximum power of 400 W at wavelength 1064 nm is used to incident the light onto a TGG crystal. The beam spot diameter is 1.3 mm

#186287 - $15.00 USD Received 4 Mar 2013; revised 8 May 2013; accepted 10 May 2013; published 31 May 2013

and the diameter and length of the crystal are 4.3 mm and 20 mm, respectively. This crystal is commercially available and gives 45 degrees Faraday rotation in an external magnetic field of 1 Tesla. The temperature profile is obtained by Eq. (2). We take 500 eigenfunction components in the thermal expansion function Eq. (2) for the numerical calculations. The convergence of the solution is satisfactory for $n \geq 20$ and $l \geq 15$. The maximum temperature rise in the TGG crystal at 300 W laser power is 4.0°C taking into account the constant beam waist throughout the TGG crystal (Rayleigh range is much greater than the length of the crystal).

Inhomogeneous temperature distribution inside the crystal results in optical path changes of propagation of light through the crystal. The most dominant effect is the change in the index of refraction due to temperature variation. There are also thermally induced strain and expansion effects which contribute to the thermal lensing effects. However, their contribution is smaller than dn/dT and they are usually ignored. [14] Once we obtain the thermal distribution, the phase difference ($\Delta\phi$) distribution, ignoring the strain and thermal expansion effects, is then given by

$$\Delta\phi(r) = k \int_0^L \frac{dn}{dT} T(r,z) dz, \tag{3}$$

where $k = 2\pi/\lambda$ is the wavevector of the incident light. The crystal refraction index gradient with temperature is shown by dn/dT. We assumed negligible variation of dn/dT with temperature throughout this work. Traditionally the phase distortion of an ideal lens with parabolic feature is fitted to the thermally induced phase difference and equivalent focal length was calculated in this manner [2, 3].

However, according to Eq. (2), the actual thermally induced phase distortion is more complex and has a complicated radial dependency. The phase difference can be obtained by integrating the thermal distribution over the crystal length, Eq. (3). The resultant phase difference is shown in Fig. 2. We also show the ideal lens phase difference obtained by fitting a quadratic function to the actual thermally induced phase difference. Quadratic function expansion of the phase difference rapidly deviates from the actual phase profile and only has a good agreement up to 35% of the beam radius while the agreement of a sextic expansion goes over 75%.

To obtain the focal length of the TGG crystal, we have made use of the diffraction theory of aberration, utilizing Strehl ratio to find the equivalent focal length of maximum normalized intensity. The Strehl ratio for a Gaussian beam is given by [15, 16]

$$\mathscr{S} = \frac{\left| \int_0^a e^{i(\Delta\phi(r) - \Delta\phi(0) + kr^2)/2f_T} e^{-r^2/\omega_0^2} r dr \right|^2}{\left| \int_0^\infty e^{-r^2/\omega_0^2} r dr \right|^2}, \tag{4}$$

where f_T is the thermally induced focal length taking into account the parabolic behavior of phase distortion in an ideal lens geometry. By maximizing the Strehl ratio for the present geometry we obtained 592 mm thermally induced focal length at 300 W laser power.

In order to obtain the beam degradation we need to take into account the higher order phase aberration in addition to the spherical quadratic behavior of an ideal lens. By inserting Eq. (2) into Eq. (3), the phase difference obtained as

$$\Delta\phi(r) \quad = \quad kL \frac{dn}{dT} \sum_n A_{n0} J_0(\nu_n r/a). \tag{5}$$

4. Effects of thermal lensing on beam quality

In order to obtain the beam quality factor we use the concept of M^2 parameter, which compares the measured laser beam profile with an ideal unaberrated Gaussian beam profile. This method

#186287 - $15.00 USD Received 4 Mar 2013; revised 8 May 2013; accepted 10 May 2013; published 31 May 2013

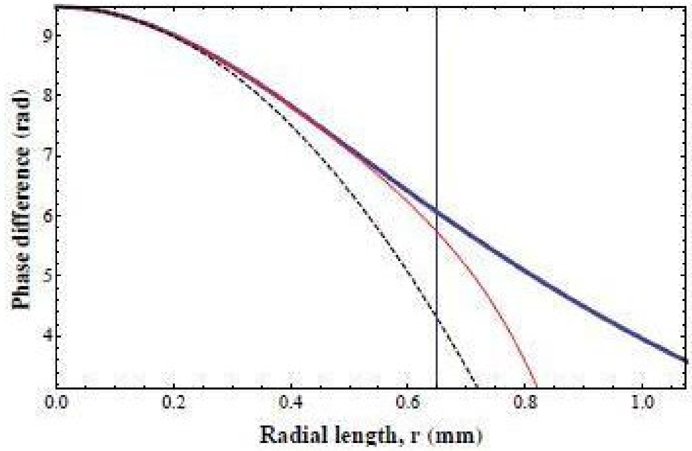

Fig. 2. An ideal lens (dashed line) and a sextic phase aberration (thin line) are fitted to the actual thermal induced phase difference (thick line). The vertical line at 0.65 mm represents a guide line for laser beam radius

starts with evaluation of second moment of the beam intensity profile across transverse direction of the beam. This method parameterizes the beam in terms of statistical measurements of intensity distribution and its spatial frequency Fourier transform. The beam waist and far field divergence of the beam are then defined in terms of the standard deviations of these statistical distributions in space and spatial frequency, respectively. [13, 17] Based on the statistical parameters, the beam quality factor, M^2, defined as

$$M^2 = \frac{\pi}{\lambda}\sqrt{(W^2\Theta^2 - S^2)}, \tag{6}$$

where W and Θ are the statistical definition for width and divergence of the beam. S is proportional to the inverse of the effective radius of curvature of the beam. A detailed description of the statistical definition of beam parameters is given in references [11, 13, 17].

To analyze and characterize the thermally induced aberrated laser beam, we make use of Zernike polynomials. Zernike polynomials are a set of orthonormal polynomials defined on a unit circle which have been used to describe the aberrations of optical systems. The advantage of using Zernike polynomials is that it takes into account all possible aberrations in a laser beam and gives analytical relations for an arbitrary degree of aberrations. In this paper, we express the phase of laser beams in terms of Zernike polynomials. Mathematically, we just change the phase expression from one orthonormal basis to the other. This transformation is possible because of the orthonormalization properties of the Zernike polynomials set. We chose those Zernike polynomials and labeling that are given by Noll. [18] The first few terms of Zernike functions expressed in polar coordinate, are listed in table 1.

The phase of the electric field of the laser beam, Eq. (5), is represented in terms of optical path difference between the thermally induced aberrated wave front beam and an ideal reference (unaberrated) beam. This phase is expanded in terms of Zernike polynomials, $Z_n(r,\theta)$

$$\Delta\phi(r) = \frac{2\pi}{\lambda}\sum_{n=1}^{N} C_n Z_n(r,\theta), \tag{7}$$

where C_n's are the coefficient of expansion. According to the azimuthal symmetry of the phase function, C_1, C_4, C_{11}, and C_{22} are the only non zero coefficients in the expansion, if we consider up to fifth-order spherical aberration. The changing of the basis from radial eigenfunctions

#186287 - $15.00 USD Received 4 Mar 2013; revised 8 May 2013; accepted 10 May 2013; published 31 May 2013

Table 1. Noll representation of Zernike polynomials [18]

Aberration	Zernike Polynomial
Piston	$Z_1(r,\theta) = 1$
Tilt	$Z_2(r,\theta) = 2r\cos\theta$
	$Z_3(r,\theta) = 2r\sin\theta$
Defocus	$Z_4(r,\theta) = \sqrt{3}\,(2r^2-1)$
⋮	⋮
3rd order spherical	$Z_{11}(r,\theta) = \sqrt{5}\,(6r^4-6r^2+1)$
⋮	⋮
5th order spherical	$Z_{22}(r,\theta) = \sqrt{7}\,(20r^6-30r^4+12r^2-1)$

of the heat equation to the Zernike eigenfunctions and considering up to fifth-order spherical aberration is equivalent to a sextic phase equation of the thermal lens induced phase distortion. The sextic phase equation for the phase expression is given by

$$\Delta\phi(r) = \frac{2\pi}{\lambda}\left(b_2 r^2 + b_4 r^4 + b_6 r^6\right), \tag{8}$$

where quadratic b_2, quartic b_4, and sextic b_6 aberration coefficients are given in terms of Zernike expansion coefficients.

$$\begin{aligned} b_2 &= 2\sqrt{3}C_4 - 6\sqrt{5}C_{11} + 12\sqrt{7}C_{22}, \\ b_4 &= 6\sqrt{5}C_{11} - 30\sqrt{7}C_{22}, \\ b_6 &= 20\sqrt{7}C_{22}. \end{aligned} \tag{9}$$

The constant term with respect to radial coordinate r has been dropped from the phase expression since it has no effect on the beam degradation. Laser light degradation of a Gaussian beam due to quartic phase aberration in a standard spherical lens is given in Ref. [10]. In this study, we consider the effect of sextic phase equation for aberration to the thermal lens induced phase distortion.

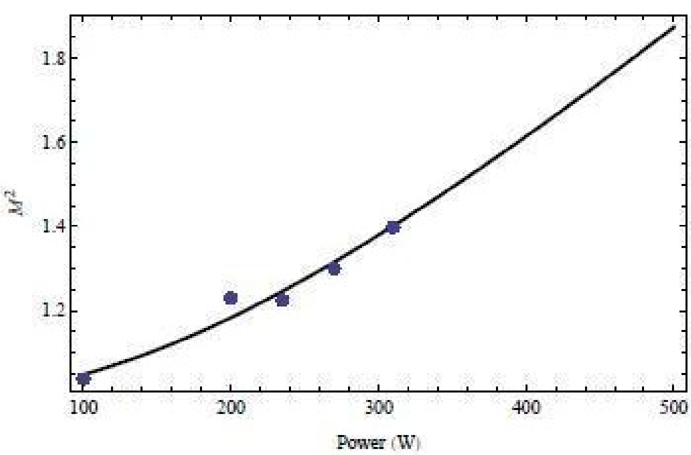

Fig. 3. Degradation in beam quality factor, M^2, as a function of input laser power for a TGG rod crystal. The theoretical curve was calculated from Eq. (10)

The degradation in a Gaussian beam quality, after propagating through the crystal rod with fifth-order spherical aberration is given by

$$M^2 = \sqrt{(M_0^2)^2 + (\Delta M_{ab}^2)^2}, \tag{10}$$

where M_0^2 is the initial beam quality before crystal rod, which we assumed a Gaussian beam. For any other arbitrary beam the initial beam quality M_0^2 is not equal one and it depends on the initial beam intensity profile. After lengthy algebra the results of calculus of moments and its Fourier transforms of the parameters in Eq. (6) provide ΔM_{ab}^2. By ignoring the higher order terms in C_{22}, we obtain ΔM_{ab}^2 as

$$\left(\Delta M_{ab}^2\right)^2 = 1440\frac{\pi^2}{\lambda^2}\left[\left(C_{11}^2 - 2\sqrt{35}C_{11}C_{22}\right)W^8 + 6\sqrt{35}C_{11}C_{22}W^{10}\right]. \tag{11}$$

We have made use of ISO11146 method to measure the beam quality after the TGG crystal in an experimental setup depicted in Fig. 1. This method is based on multipoint beam waist fitting procedure which involves recording of the beam waist at different positions along the beam propagation path. [19] The beam waist of any arbitrary laser beam evolves quadratically with distance along the axes of propagation. Therefore, We can obtain the beam waist profile by fitting a quadratic polynomial to the experimental beam waist data

$$\omega^2(z) = Cz^2 + Bz + A, \tag{12}$$

with the angular spread defined as $\theta = \sqrt{C}$, the minimum beam spot size as $\sqrt{A - B^2/4C}$, and the position of the beam spot as $-B/2C$. Having the beam waist profile, one can get the beam quality factor from $M^2 = \pi\omega_0\theta/\lambda$. The experimental error for M^2 is less than 4%.

The calculation of M^2 versus laser power through the TGG crystal has been done with the help of an in-house coding in Mathematica environment. The result is shown in Fig. 3 along with experimental measurement. For 300 W beam power, the beam quality factor increases from 1 to 1.4 or produces beam degradation ΔM_{ab}^2 from zero to 1. For TGG crystal with very low absorption (0.0015 cm^{-1}) and laser power up to 300 W, the fifth order aberration effects remain small and slightly degrades the beam quality. However, beam quality deteriorates rapidly with increasing power. At 500 W, M^2 approaches 2 and grows exponentially with power. In addition to laser beam power and beam size, the crystal size, crystal absorption and thermal conductivity also have an effect on M^2. At the Gaussian beam waist of 1.3 mm diameter, M^2 of a TGG crystal rod with 4.3 mm diameter and 20 mm length varies exponentially with power according to the following fitting function to the theoretical curve, $M^2 \approx \exp(P/840)$.

5. Conclusion

An analytical expression for the beam quality factor, M^2 of a high power laser beam incident on an edge-air-cooled TGG rod crystal has been derived. This analysis can also be applied to the other optical crystals incident by high power lasers. This study gives an idea for the diffraction limit of the beam quality in design of a high power optical isolator taking into account the beam degradation. A high power laser beam diverges more rapidly with distance than the original beam before TGG crystal as M^2 grows with the laser power. Several quantities, from both optical crystal parameters and beam parameters, were found to have direct effects on beam quality. A simple relation of M^2 versus laser power was found for the specific situation of this study. This analysis can easily be extended for any other optical systems showing thermally aberrated effects involving, for example, a top-hat intensity profile of incident light. In this case, the initial beam quality M_0^2 is no longer equal to 1 and its effect on thermal profile and beam quality can be calculated from Eqs. (2) through (6).

#186287 - $15.00 USD Received 4 Mar 2013; revised 8 May 2013; accepted 10 May 2013; published 31 May 2013